A new approach to enhancement of frequency bandwidth of surface seismic data

Satinder Chopra+ and Vladimir Alexeev+

Introduction

It is a common observation that seismic waves propagating through the earth are attenuated. As these elastic waves travel deeper they lose energy, in contrast to spherical spreading, where energy is spread over a wider area, and reflection and transmission of energy at interfaces, where its redistribution occurs in the upward or downward directions. This loss is frequency dependent: higher frequencies are absorbed more rapidly than lower frequencies, such that the highest frequency usually recovered on most seismic data is about 80 Hz. Moreover, absorption appears to vary with the lithology of the medium. The unconsolidated near-surface absorbs more energy than the underlying compact rocks. In the extreme case most of the energy may be absorbed in the first few hundred metres of the subsurface. It is therefore important to study absorption and to determine ways in which it can be detected in seismic data.

Attenuation of seismic waves

Understanding of the attenuation properties of the earth is important for two reasons. Firstly, because as seismic waves propagate through the subsurface, their amplitudes are reduced. Secondly, because attenuation characteristics, when determined, reveal useful information such as the lithology and the degree of saturation of rocks. However, it should be pointed out that the phenomenon of attenuation is more complex than the elastic aspects of seismic-wave propagation. It is not easy to make measurements in the laboratory or in the field. There are numerous mechanisms contributing to attenuation, and changes in some of the conditions can affect attenuation significantly (Toksöz and Johnston 1981).

One commonly used measure of attenuation is the attenuation coefficient α, which is the exponential decay constant of the amplitude of a plane wave propagating in a homogeneous medium. The amplitude of a plane wave propagating in a homogeneous medium may be given as

$$A_r = A_0 \exp(-\alpha r), \tag{1}$$

where A_r is the amplitude at any distance r from the source, A_0 is the initial or reference amplitude and α is the attenuation coefficient, is given by

$$\alpha = \frac{\pi f}{QV}, \tag{2}$$

where Q is the seismic quality factor and is the other commonly used measure of attenuation, V is the velocity and f is the frequency. The seismic quality factor Q is defined as

$$Q = \frac{2\pi}{\text{Fraction of energy lost per cycle}},$$

or

$$Q = \frac{2\pi}{\Delta E / E}.$$

Using equation (1) to substitute for $\Delta E / E$ for a single cycle, it can be shown that

$$Q = \frac{\pi}{\delta}, \tag{3}$$

where δ is the logarithmic decrement and is defined as the natural logarithm of the ratio of the amplitudes of two consecutive cycles, i.e.

$$\delta = \ln\left\{\frac{\text{amplitude}}{\text{amplitude one cycle later}}\right\} = \alpha\lambda = \frac{\alpha V}{f},$$

which leads to equation (2).

Laboratory and *in situ* measurements show that Q correlates with rock type, fluid type and degree of fluid saturation and thus the estimation of Q is a potential diagnostic for reservoir characterization. Most sedimentary rocks have a value of Q ranging from 20 to 200 (Sheriff and Geldart 1995), the lower values of Q indicating higher attenuation and vice versa. Reliable estimates of Q could assist greatly in understanding the lithology of subsurface rocks. Several investigators have demonstrated the computation of Q from seismic and VSP data. Q estimates could be used to determine the levels of fluid/gas saturation (Winkler and Nur 1979; Wyllie *et al.* 1962; Gardner *et al.* 1974), because Q could be an order of magnitude more sensitive to changes in saturation or pore pressure than velocity. Geophysicists have attempted to determine attenuation from subsurface data and then apply corrections for it.

Compensating for attenuation

Deconvolution

Different conventional procedures are adopted to compen-

+ *formerly at Core Laboratories Reservoir Technologies Division, Calgary.*

sate for frequency attenuation. A common practice has been to use a two- or three-window statistical deconvolution to correct for the dynamic loss of high frequencies. This involves choosing two or three time-windows for the deconvolution, each with its own parameters, keeping the time-variant nature of the embedded source wavelet in mind. These windows are usually made to overlap to avoid artefacts. However, there are problems with this approach: the filters must be derived from smaller windows, which are less likely to meet the statistical assumptions, and these windowed zones often exhibit phase distortions at the point of overlap.

Time-variant spectral whitening

The other method is to use time-variant spectral whitening (TVSW). The method involves passing the input data through a number of narrow band-pass filters and determining the decay rates for each frequency band. The inverse of these decay functions for each frequency band is applied and the results are summed. In this way, the amplitude spectrum for the output data is whitened in a time-variant way. The number of filter bands, the width of each band and the overall bandwidth of application are the different parameters that are used and adjusted for an optimized result (Yilmaz 2001). In this method, the high-frequency noise is usually amplified and so a band-pass filter must be applied to the resulting data. Since it is a trace-by-trace process, TVSW is not appropriate for AVO applications.

Inverse Q-filtering

If we had an analytic form for an attenuation function, it would then be easy to compensate for its effects. Thus, in practice, attempts are first made to estimate a Q-model for the subsurface. Inverse Q-filtering is then carried out, removing the time-variant wavelet effects by absorption and broadening the effective seismic bandwidth by correcting the loss of high-frequency signal. These attempts have met with a varying degree of success, depending on the assumptions used in the particular approach and how well they are met in practice.

Determination of Q

Seismic data

A large body of work exists for the determination of Q from seismic data (Raikes and White 1984; White 1993; Dasgupta and Clark 1998) and VSP data (Hauge 1981; Pujol and Smithson 1991). It is not the purpose of this paper to discuss the different techniques that can be used for the determination of Q; however, the methods that have been studied include spectral ratios, matching filters, centroid frequency shift and instantaneous frequency (Tonn 1991; Raikes and White 1984). Another class of algorithms exists, where inverse Q-filtering is viewed as a migration like procedure, i.e. backward propagation of the recorded wavelet. The Q-filter can then be removed from the surface-recorded data by a downward-stepping through each step (Hale1982; Hargreaves *et al.* 1987)

The spectral-ratio method is commonly used for Q computation. Different frequency components are attenuated at different rates, and attenuation is indicated by changes in the amplitude of various frequency components or spectral ratios with time.

The amplitude spectrum $A(z,f)$ of the trace from a level z is assumed to decay exponentially from a reference amplitude $A(z_0,f)$ at level z_0, i.e.

$$A(z,f) = A_0(z_0,f)\exp\left[-\alpha(z-z_0)\right]. \quad (4)$$

This gives

$$\ln\frac{A(z,f)}{A_0(z_0,f)} = -\alpha(z-z_0)$$

$$\ln\frac{A(z,f)}{A_0(z_0,f)} = -\frac{\pi(T-T_0)}{Q},$$

or

$$Q = -\frac{\pi(T-T_0)}{\text{Slope}} \quad \text{where Slope} = \frac{\ln\frac{A(z,f)}{A_0(z_0,f)}}{f}, \quad (5)$$

T and T_0 being the first-arrival times at levels z and z_0, respectively.

Thus the slope of the variation of the natural logarithm of the spectral ratio versus frequency (which is expected to be linear) is computed. As this estimation of slope has a direct bearing on the computed Q-values, its accurate determination is important. In practice, however, a bias is usually introduced in the least-squares fitting techniques by the spectral nodes (the individual points on the graph of natural logarithm of spectral ratio versus frequency) and so departures from linearity are usually observed on spectral-ratio plots (Oliver 1992). In addition, data that is free from interference (contamination with extra arrivals) is never obtained, and so wave spectra that contain effects of interference, e.g. a ringing effect or the effect of wave modes leading to inaccurate Q-values, are used. Spectral-ratio-based Q-estimates are also sensitive to the taper type used to window the data (Pujol and Smithson 1991).

VSP data

It is well known that VSP data records higher frequency data than surface seismic data. This is because the energy recorded by the VSP traverses the unconsolidated weathering zone just once. Spencer *et al.* (1983) computed spectral ratios in VSPs between each direct arrival waveform and the direct arrival at some reference depth. They estimated interval Qs by measuring the slope of linear segments on the resulting cumulative attenuation versus depth plots. Apart from the

bias introduced during least-squares fitting on spectral nodes, this method has another interesting shortcoming. The full range of VSP depth levels is often found not to be useful for computation of Q by the spectral-ratio method (Xu *et al.* 2001). Negative Q-values are frequently obtained in some usually shallow intervals which do not have a physical explanation. One of the reasons cited in the literature for obtaining negative Q-values using the spectral-ratio method is due to the choice of short depth intervals, as estimates tend to become stable at larger depth intervals (Spencer *et al.* 1982; Raikes and White 1984). This leads to an unavoidable trade-off between resolution and accuracy (Harris *et al.* 1997).

New method for attenuation correction

A new method called High-Frequency Restoration (HFR) has been developed by Paradigm Geophysical for the determination of attenuation from VSP data and its application to surface seismic data. It utilizes the frequency decay experienced at different VSP depth levels in a well.

For the VSP downgoing signals, the ratio of the change in trace frequency at successive depths describes the decay of frequency components between those observation points. The change in the trace amplitudes and the length of the first-arrival wavelets at successive depth levels is used to estimate the change in the frequency components. An inverse operator (in the time domain) is then designed to compensate this change. For successive depth levels, a suite of such operators is generated. As the computed operators determine the change in frequency of the first arrivals between successive depth levels, the inverse operators compensate for both the attenuation and the dispersion that may cause a lowering of the frequency of the VSP first-arrival wavelets. For application to surface seismic data, the time-window of application is first determined by correlating the available log data, the aligned upgoing VSP data and the seismic data. The theory behind this computation and the application details can be found in Chopra et al. 2003.

The HFR procedure, when run on the seismic data, has an effect similar to a time-varying attenuation correction. As operators are applied continuously to the stacked data, windowing is avoided. Since no computation similar to the spectral-ratio method is employed, a negative-Q type situation does not arise, nor are there any sensitive issues pertaining to taper types. Application of these inverse operators on surface seismic data enhances the frequency bandwidth by restoring the attenuated frequency components.

As the operators are derived from the downgoing wavefield, their performance is dependent on the quality of the VSP data. For instance, poor VSP source repeatability and variations in geophone coupling with depth could prove detrimental to the performance of the HFR application. However, with the present available VSP acquisition technology and with caution exercised during acquisition of data, good data quality can be ensured and subsequently satisfactory application of HFR.

Applications

Application of the HFR procedure described above has been evaluated for various subsurface configurations in the context of hydrocarbon exploration. Some examples are given below, which illustrate the advantages of adopting the HFR procedure.

Figure 1(a) shows an in-line section extracted from a 3D migrated seismic data volume from central Alberta. The zone of interest is the Lower Mannville sandstone interval at a depth of 1300 to 1350 m. Surface seismic data is expected to assist in defining sand presence and porosity development in this interval (940–1000 ms). A close look at the interval of interest indicates that there is no reflection detail to interpret. The bandwidth of the seismic data is 8–50 Hz.

Spectral whitening was applied to the migrated surface seismic volume to enhance the frequency bandwidth. Next, the spectral-ratio method was used to determine Q-values from VSP data and inverse Q-filtering was carried out on prestack data, which were then migrated.

Finally, the HFR procedure was applied to the original migrated seismic data volume. The objective was to obtain a comparative evaluation of the performance of the three different processes. In Figure 1, the input seismic line is compared with each of the above outputs. Focusing on the broad zone of interest, an improvement can be seen in the reflection detail after each of these processes; however, while spectral whitening tends to increase the noise as well as improve the signal (more-or-less continuous reflection detail as indicated), the Q-compensated section appears to have less effect. The HFR section appears to have a controlled action in the sense that the amplitudes appear to vary along the indicated reflectors.

In further investigation, the four volumes were inverted for acoustic impedance. Figures 2 and 3 show the time and the horizon slices at the sandstone level from each of these volumes. The following observations can be made:

(i) Figures 2(a) and 3(a): There is not much variation in the high impedance patterns, possibly due to poor bandwidth (resolution) of the input seismic data.
(ii) Figures 2(b) and 3(b): The high impedance patterns do not quite follow the patterns seen in Figs 2(a) and 3(a).
(iii) Figures 2(c) and 3(c): The spectrally whitened impedance slices have no variation within the high impedance patterns, as mentioned above, as both the signal and noise are enhanced to high levels.
(iv) Figures 2(d) and 3(d): The HFR impedance slices show a variation within the high impedance patterns and follow the overall high impedance pattern in Figs 2(a) and 3(a).

Usefulness of the method

The high-frequency restoration of surface seismic data has also been evaluated by running the Coherence Cube (Core Laboratories) analyses on the seismic volumes before and after HFR. Figure 4 shows the seismic representation of a reef, before and after filtering. The boundary of the reef can-

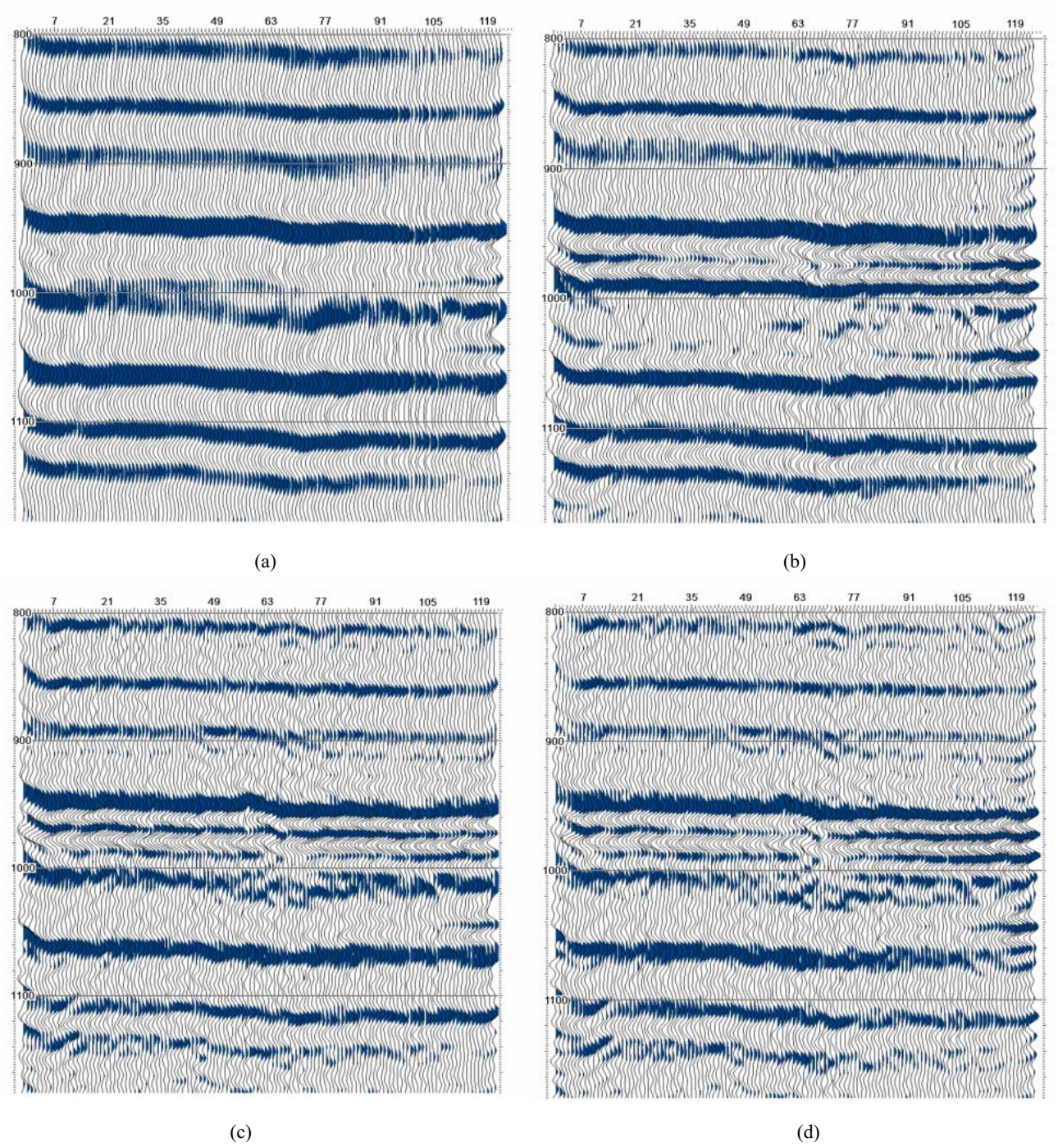

Figure 1 *Sections of an in-line survey from a 3D seismic data volume which have been processed for enhanced frequency bandwidth. (a) Input seismic line; (b) after inverse Q-filtering; (c) after spectral whitening; (d) after HFR.*

not be seen clearly on the horizon slice from the Coherence Cube before HFR application, but appears quite clearly on the Coherence Cube horizon slice after HFR.

Acoustic impedance inversions were performed on the seismic volumes before and after HFR processing. Inversion algorithms generally assume a stationary wavelet in the convolutional model of the seismogram. This is often satisfactory if the time-window of the inversion is not too long. It might be expected that any processing that can remove the predictable time-varying wavelet decay due to earth transmission processes would contribute to the 'stationarity' of the wavelet, though it is not always the case. Wavelets extracted from different time-windows of a seismic line after HFR processing are found to be stable (Chopra 2003). Obvious differences in inversion that stem from the greater

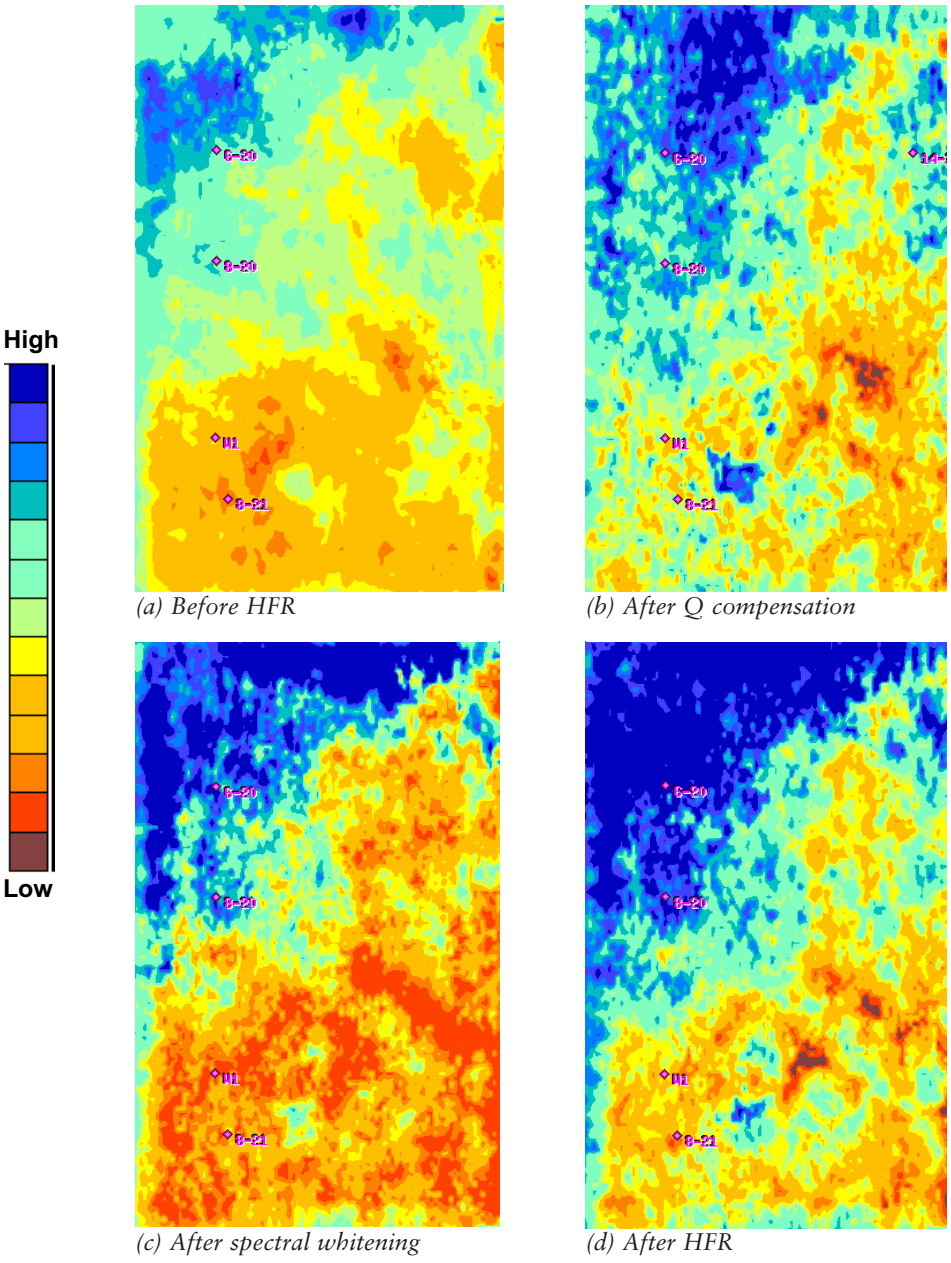

Figure 2 *Time slices from different volumes. Application of the conventional procedures for frequency enhancement does not preserve amplitudes. Note the preservation of amplitudes on HFR impedance inversion*

stability of the seismic wavelet can be observed on HFR impedance sections after HFR processing.

Impedance inversion performed on data with a larger bandwidth also yields more information than with a poor bandwidth. For example, features that cannot be detected on seismic inversion results before *Q* deconvolution are clearly visible afterwards and so enable a detailed interpretation of important stratigraphic features (Hirsche *et al*. 1984). Figure 5(a) shows segments of an impedance section. A gas-producing well W is seen intersecting the highlighted portion corresponding to a gas sand. However, the green streak continues across the segment and does not identify the gas sand. The HFR procedure was run on the seismic section and impedance inversion was carried out (Fig. 5b). Note the dark green streak (low impedance, within the highlighted portion) seen clearly representing the gas sand. This example thus amply corroborates the findings similar to those of Hirsche *et al*. (1984), using HFR.

Robustness of the method

An important element that lends strong support to the usefulness of any procedure is its robustness. A valid concern when adopting such a procedure would be to examine the effect of HFR filters away from the borehole where they are determined. Tests carried out on the determination of filters in different wells in an area (assuming the data quality is good and is acquired using similar equipment) have yielded almost identical filter sets (Chopra *et al*. 2003). However, a visual correlation of well data with surface seismic data before and after HFR would be more convincing.

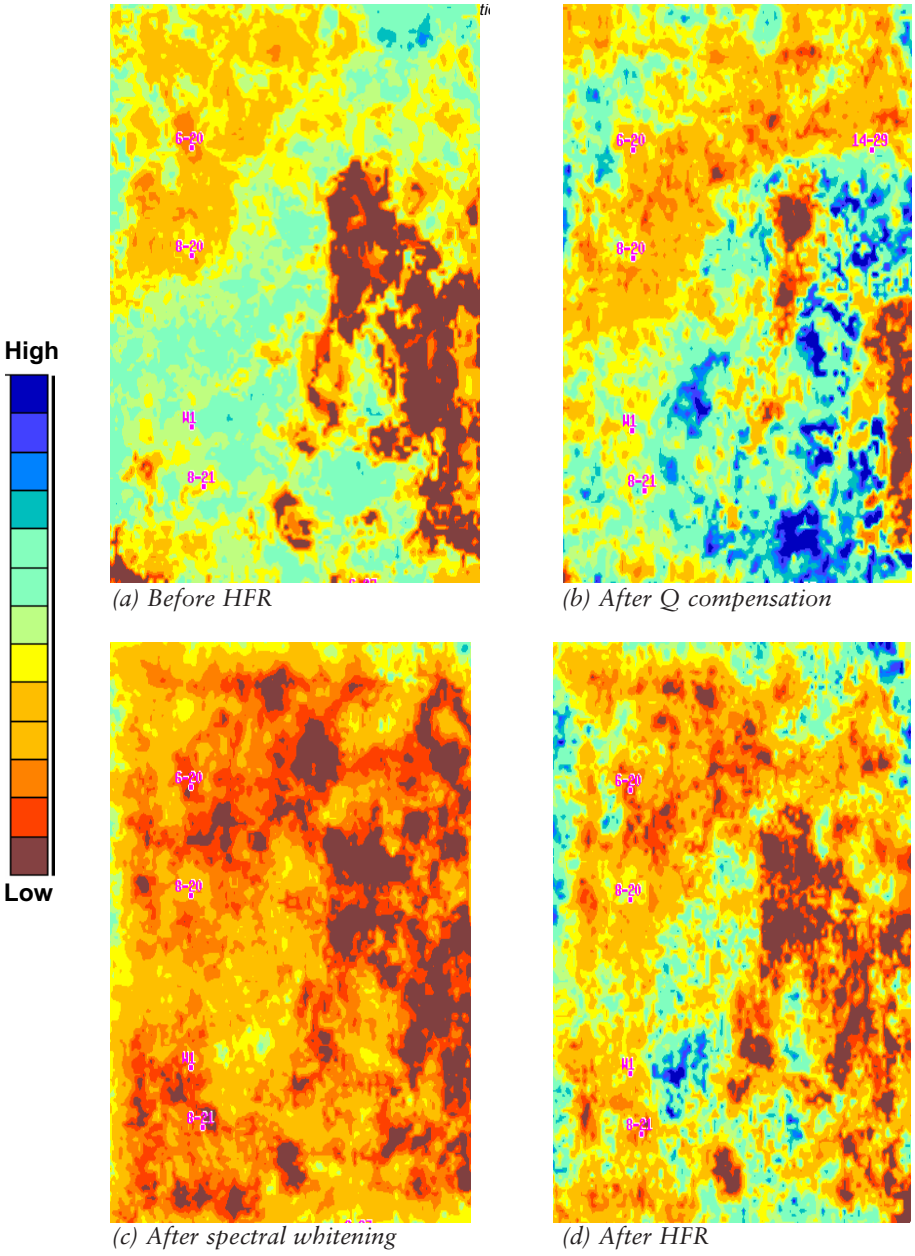

(a) Before HFR (b) After Q compensation

(c) After spectral whitening (d) After HFR

Figure 3 *Horizon slices from different volumes. Application of any of the conventional procedures for frequency enhancement does not preserve amplitudes. Note the preservation of amplitudes on HFR impedance inversion.*

Example 1

A zero-offset VSP was recorded in well C, which is situated within a 3D seismic survey area covering a producing field in southern Alberta. The objective at the time of the VSP data acquisition was to obtain accurate velocity information in the area, which would enable good well ties and help in the stratigraphic interpretation of the surface seismic data. Well log data was available for two other wells, A and B, in the survey area. Well A is close to well C (<100 m), but well B is about 600 m away from both A and C.

The VSP data was processed to derive the HFR filters from the downgoing VSP wavefield as explained above, and the separated upgoing VSP wavefield was used to process a corridor stack. Figure 6 shows an in-line section and a cross-line section from the 3D surface seismic volume (passing through well C) with the corridor stack, synthetic seismogram and sonic log curve overlaid on them.

HFR was run on the 3D seismic volume and the same synthetic seismogram and sonic log curve were overlaid on the in-line and cross-line sections shown in Fig. 6(a). Note the distinct improvement in resolution and the continuity of the reflection events. Due to poor resolution before HFR, some of the reflection events were not sufficiently visible to match them with their corresponding events on the well data. After HFR there is a much better correlation between these reflection events.

Since the HFR procedure was run over the whole 3D volume and since there are no significant dips in the area, it was expected that the seismic data after HFR would correlate well with the log data in the other two wells. Figures 7 and

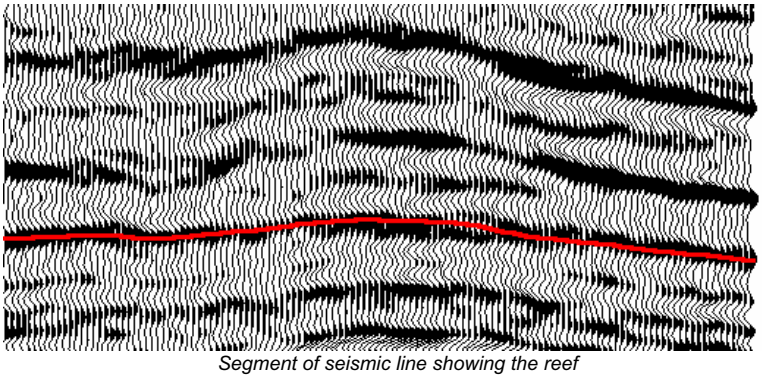

Segment of seismic line showing the reef

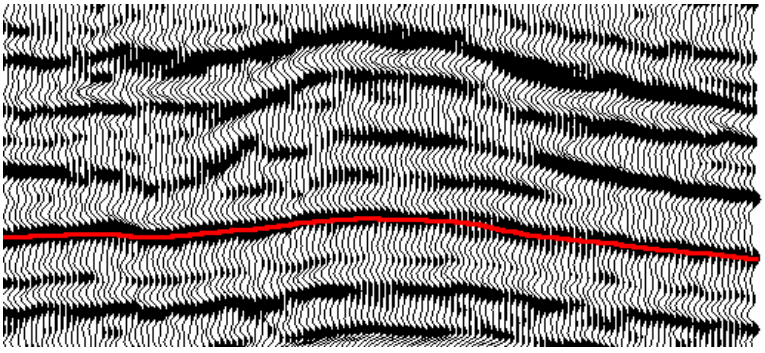

Segment of seismic line after HFR processing showing the reef

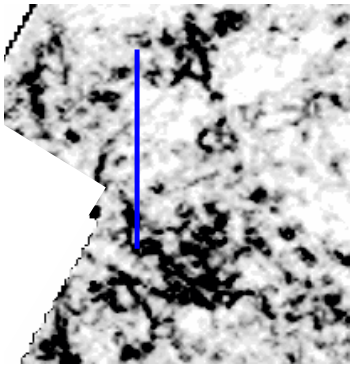

Reef not seen clearly on coherence horizon slice

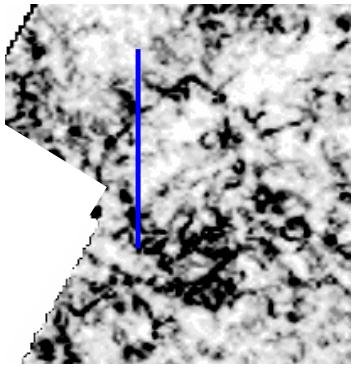

Reef seen clearly on coherence horizon slice after HFR processing

Figure 4 *Seismic representation of a reef, before and after HFR filtering.*

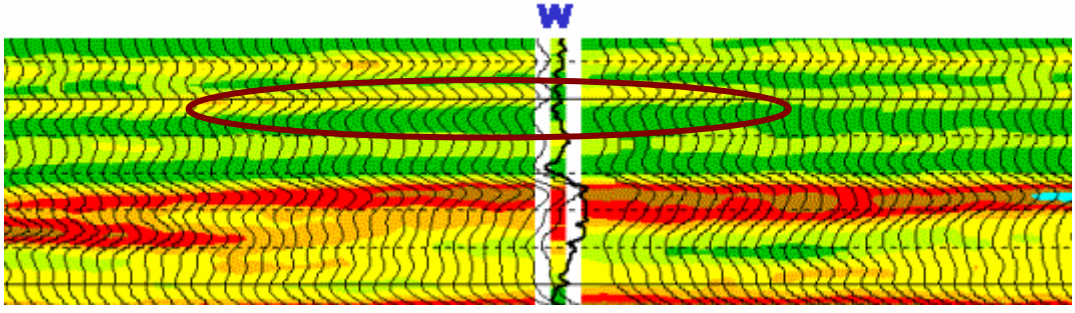

(a): Segment of impedance section. Highlighted portion indicates lower impedance at the level of gas sand but does not distinguish it.

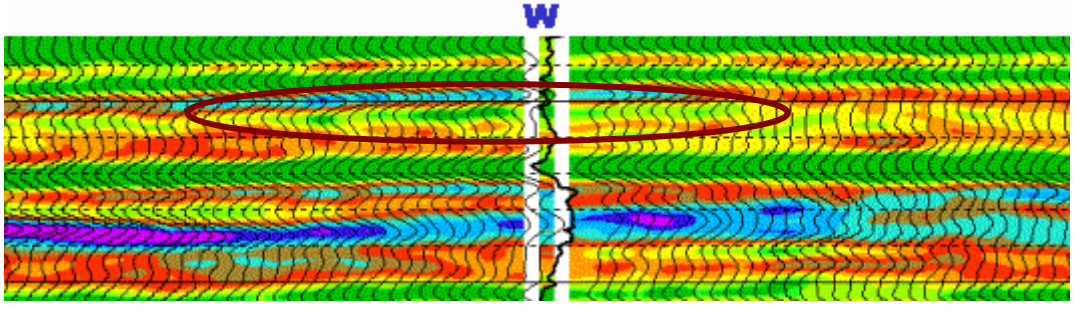

(b): Segment of impedance section. Highlighted portion indicates the extent of the gas sand clearly

Figure 5 *Segments of the impedance section for a seismic profile passing through a producing gas well.*

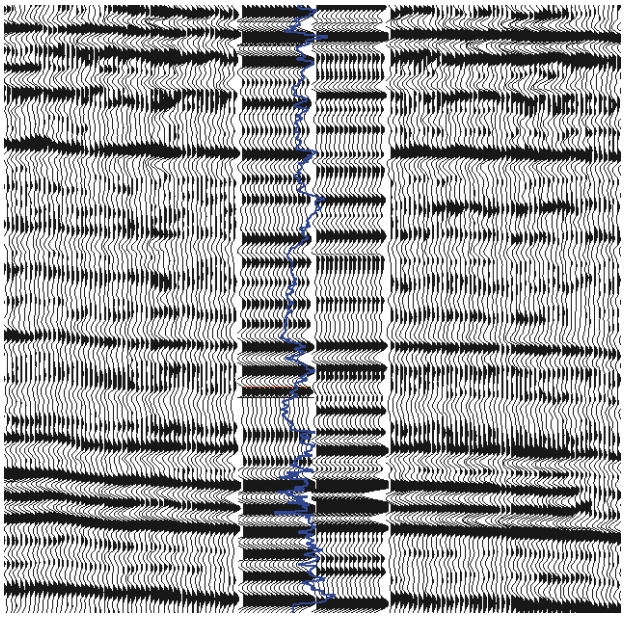

Synthetic Corridor
Bandpass filtered 12-15-55-60

Corridor stack, synthetic seismogram & sonic curve for well C overlaid on seismic inline

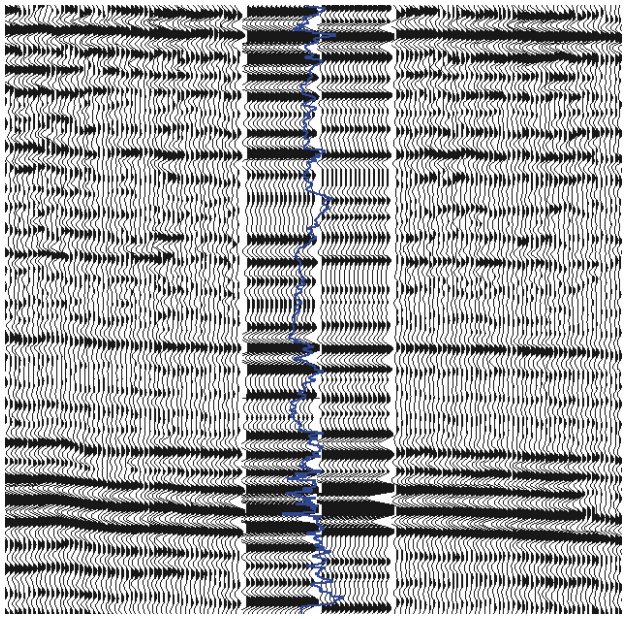

Synthetic Corridor
Bandpass filtered 12-15-65-70

Corridor stack, synthetic seismogram & sonic curve for well C overlaid on seismic inline after HFR

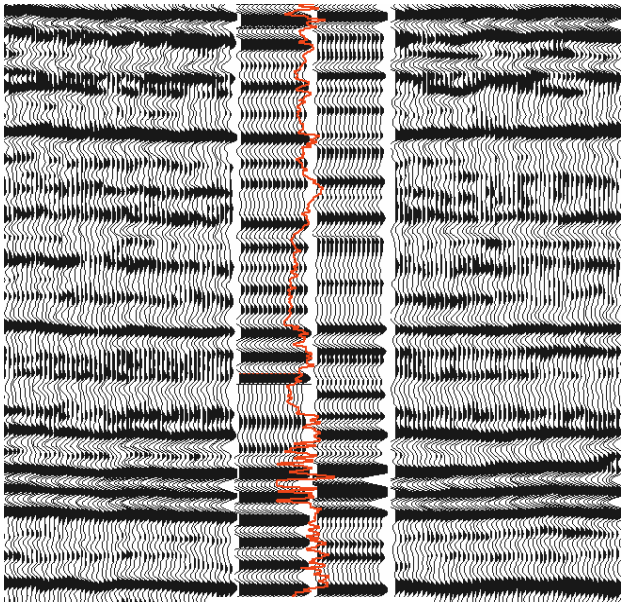

Synthetic Corridor
Bandpass filtered 12-15-55-60

Corridor stack, synthetic seismogram & sonic curve for well C overlaid on seismic cross-line

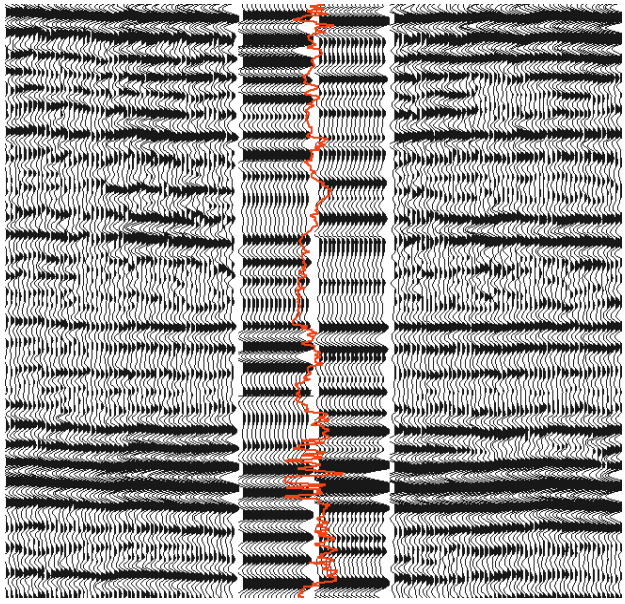

Synthetic Corridor
Bandpass filtered 12-15-65-70

Corridor stack, synthetic seismogram & sonic curve for well C overlaid on seismic cross-line after HFR

Figure 6 *In-line and cross-line sections from the 3D surface seismic volume (passing through well C) with the corridor stack, synthetic seismogram and sonic log curve overlaid on them.*

8 show the correlation of synthetic seismograms and sonic log curves for wells A and B. Clearly, the well data tie reasonably well with seismic after HFR.

This observation corroborates the conclusion stated above: that the HFR procedure has an effect similar to time-variant attenuation correction, and achieves the desired correction away from the position where this correction is determined. This conclusion has significant applications in that

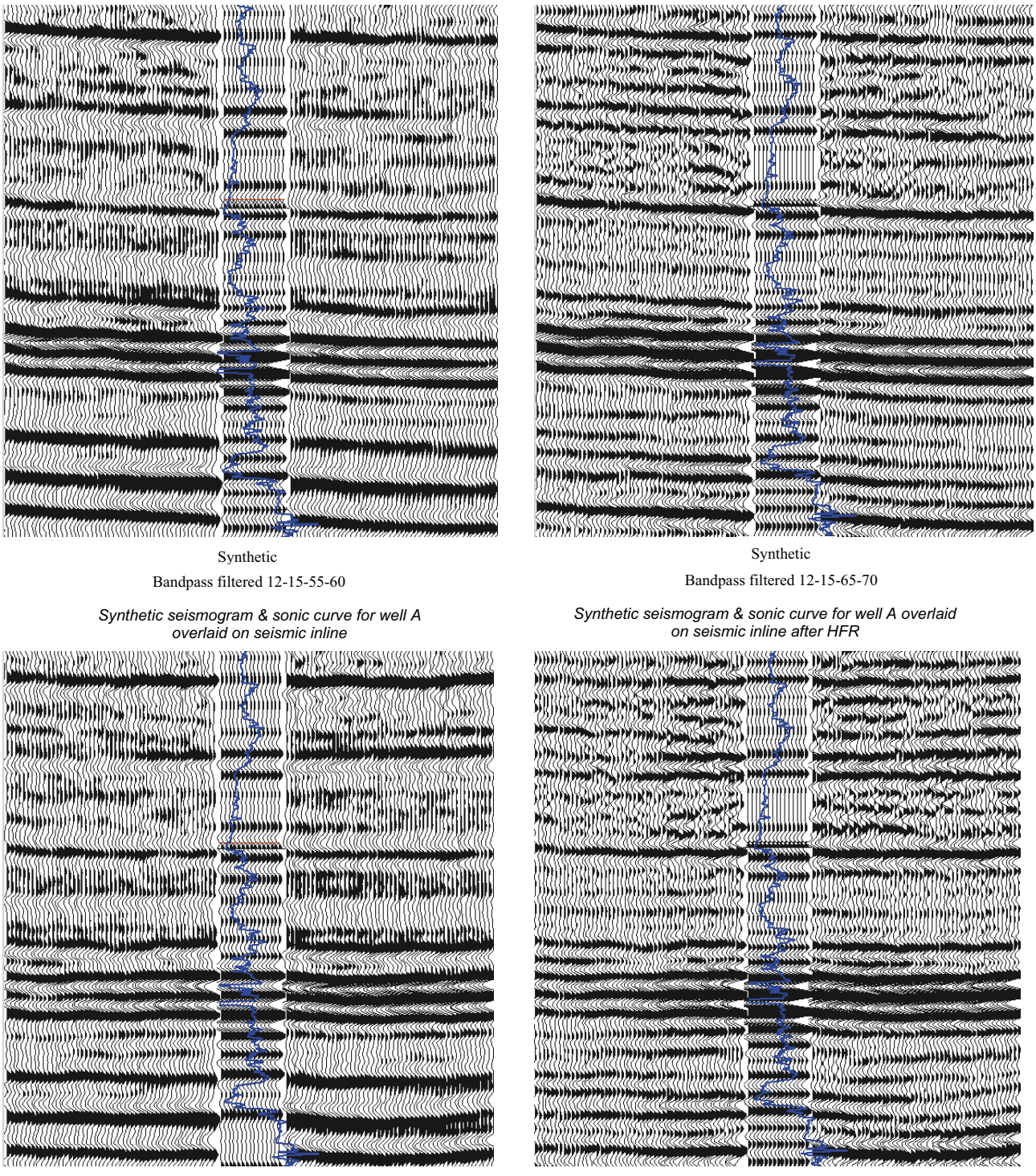

Figure 7 *Correlation of synthetic seismogram and sonic log curve for well A.*

more accurate interpretations can be carried out on data with higher resolution.

Example 2

Figure 9 shows another example, in which the corridor stack and sonic log curve for well D are overlaid on a segment of a seismic section for an area in the Middle East. Both the corridor stack and the sonic log curve have been filtered back (8–12–45–50 Hz) to match the frequency bandwidth of the seismic. Note the poor correlation in the zone where there is no reflection detail. After application of HFR to surface seismic data, the resolution and continuity of reflection events is enhanced and there is now far better correlation with the well data (now filtered to 8–12–65–70 Hz). Figure 10 shows

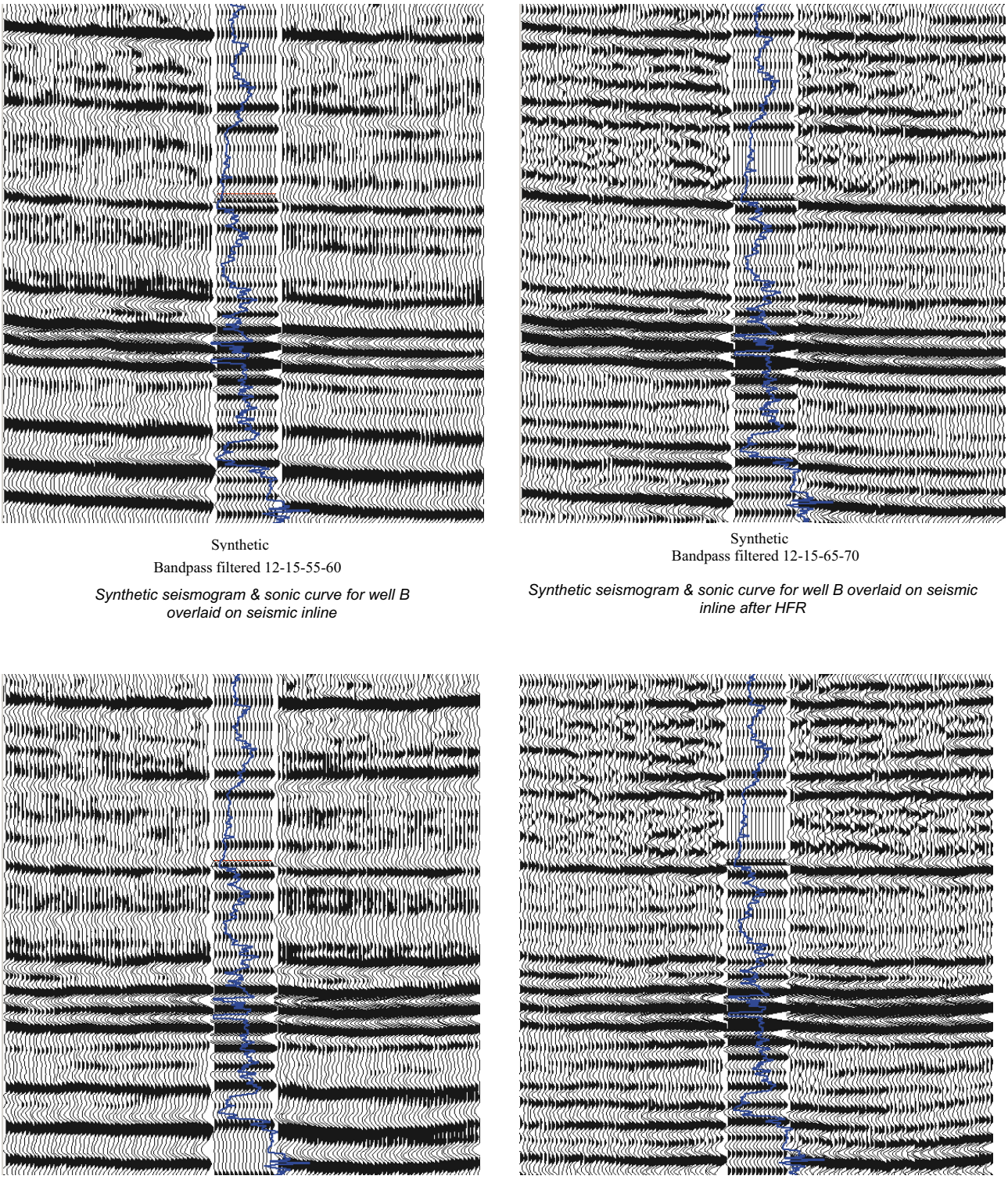

Figure 8 *Correlation of synthetic seismogram and sonic log curve for well B.*

a similar correlation for well E in the same area, about 12 km from well D (log data available over only the portion shown). Clearly, any stratigraphic interpretation carried out on HFR run data is bound to be more accurate. Such tests, carried out on different wells in different areas, lead us to the conclusion that the HFR method is robust. For areas where the geology changes fast laterally, it may be necessary to follow a space adaptive filter application approach.

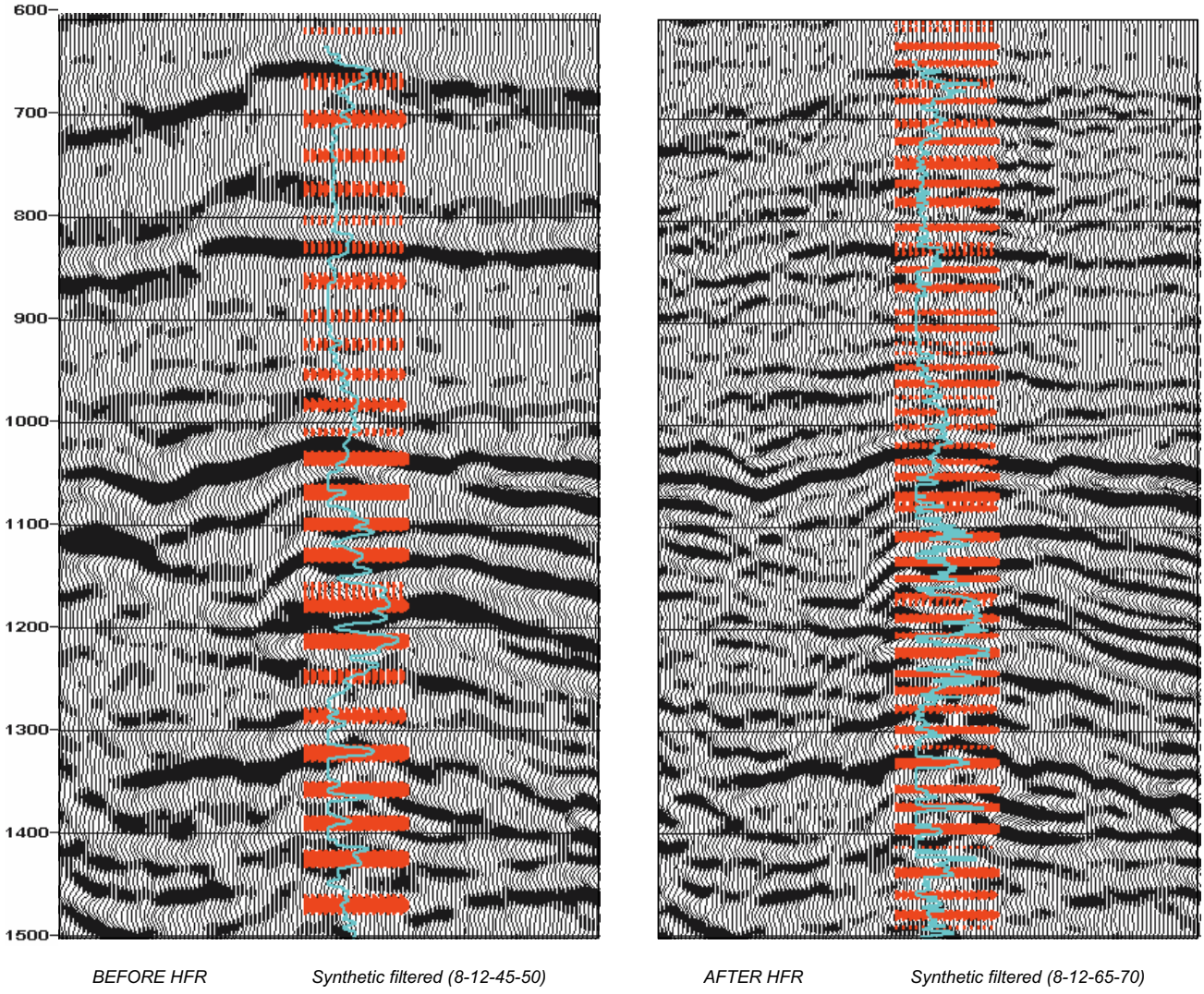

Figure 9 *Corridor stack and sonic curve for well D overlaid on seismic in-line section.*

Conclusions

HFR methodology consists of determining the decay in frequency using the downgoing VSP first arrivals from successive depth levels and then applying the inverse decay function to subsurface seismic data. This allows us to take advantage of the higher resolution and signal-to-noise ratio of VSP data and enhance the bandwidth of seismic data. This procedure is robust and helps to define trends better, leading to more confident interpretations. Our applications illustrate the usefulness of the procedure, and could redefine prospects, which in some cases have been declared unsuccessful when based on interpretation of seismic data with poor bandwidth. The application of the new method to post-stack data is illustrated here. Application to prestack data is also very effective and its effectiveness in AVO analysis will be discussed separately elsewhere.

Acknowledgements

We are grateful to Vasudhaven Sudhakar for encouraging this work. We thank Core Laboratories for permission to publish this paper. We also thank ConocoPhillips, Canada and WesternGeco for permission to show their data. Finally, we offer our appreciation to the reviewers of the paper for their constructive comments, which have improved its overall quality.

References

Chopra, S. [2003] Enhancing seismic frequency bandwidth using VSPs – a case study. *Oil and Gas Journal* Oct. 20, p.38.

Chopra, S., Alexeev,V. and Sudhakar,V. [2003] High frequency restoration of surface seismic data. *The Leading Edge* **22**, 730–738.

Dasgupta, R., and Clark, R.A. [1998] Estimation of Q from surface seismic reflection data: *Geophysics*, **63**, 2120-2128.

Gardner, G.H.F., Gardner, L.W. and Gregory, A.R. [1974] Formation velocity and density - The diagnostic basics for stratigraphic traps. *Geophysics* **39**, 770–780.

Hale, D. [1982] Q-adaptive deconvolution. 52nd SEG

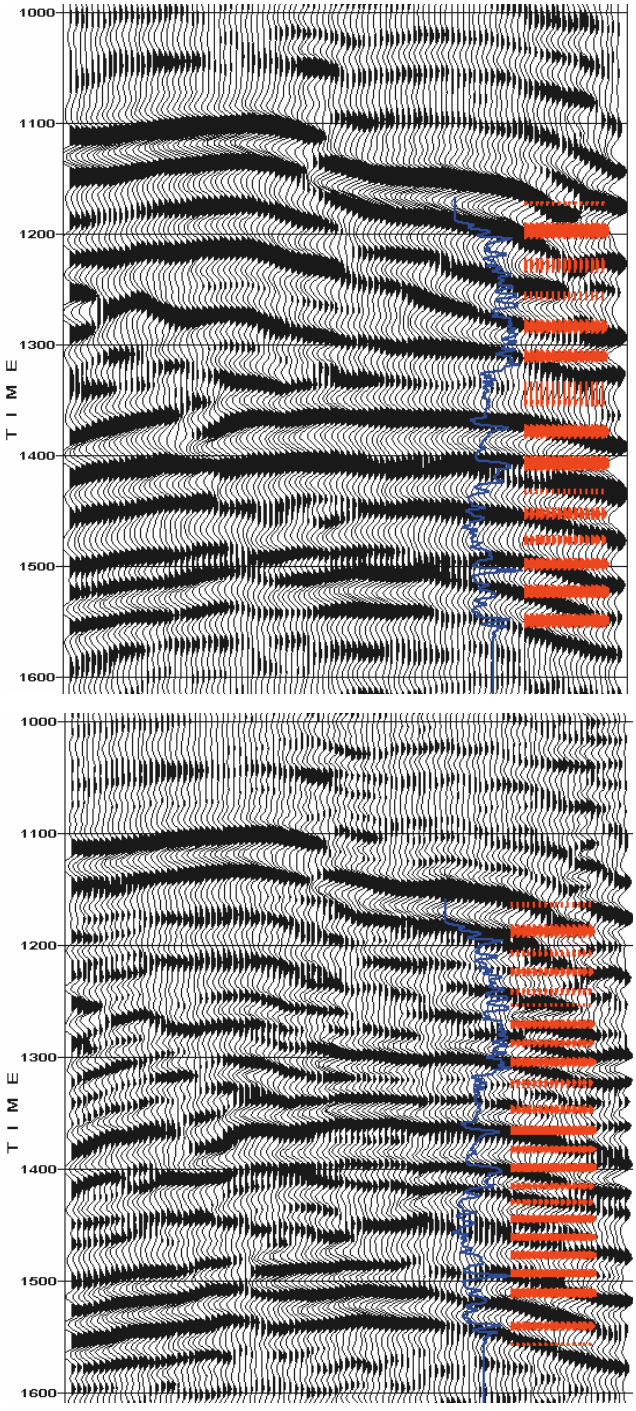

Figure 10 *Synthetic seismogram and sonic curve for well E overlaid on seismic in-line section after HFR.*

Meeting, Dallas, USA, *Expanded Abstracts, Session: S6.7.*
Hargreaves, N. D., Calvert, A.J. and Hirsche, W.K. [1987] A fast inverse Q-filter. 57th SEG Meeting, New Orleans, USA, *Expanded Abstracts, Session: POS1.7.*
Harris, P.E., Kerner, C., and White, R.E. [1997] Multichannel estimation of frequency-dependent Q from VSP data. *Geophysical Prospecting* **45**, 87–110.
Hauge, P.S. [1981] Measurements of attenuation from vertical seismic profiles: *Geophysics,* **46**, 1548-1558.
Hirsche, W.K., Cornish, B.E., Wason, C.B. and King, G.A. [1984] Model-based Q compensation. 54th SEG Meeting, Atlanta, USA, *Expanded Abstracts, Session: S18.7.*
Oliver, J.S., [1992] Robust P-wave attenuation measurements from VSP first arrivals: 54th EAEG Annual Conference, Paris, *Expanded Abstracts,* Paper P067, 582-583.
Pan, C. [1998] Spectral ringing suppression and optimal windowing for attenuation and Q measurements. *Geophysics* **63**, 632–636.
Pujol, J., and Smithson, S. [1991] Seismic wave attenuation in volcanic rocks from VSP experiements: *Geophysics,* **56**, 1441-1455.
Raikes, S.A. and White, R.E. [1984] Measurements of earth attenuation from downhole and surface seismic recordings. *Geophysical Prospe*cting **32**, 892–919.
Sheriff, R.G. and Geldart, L.P. [1995] *Exploration Seismology* (2nd ed.). Cambridge University Press.
Spencer, T.W., Davis, F.E., Wu, R.C. and Zeitvogel, M. [1983] VSP measurement of seismic attenuation. 53rd SEG Meeting, Las Vegas, USA, *Expanded Abstracts, 590–592*
Spencer, T.W., Sonnad, J.R. and Butler, T.M. [1982] Seismic Q – stratigraphy or dissipation? *Geophysics* **47**, 16–24.
Toksoz, M.N. and Johnston, D.H. [1981] Seismic Wave Attenuation, Geophysics Reprint Series No. 2,339-351.
Toksöz, M.N. and Johnston, D.H. [1981]
Toksöz, M.N., Johnston, D.H. and Timur, A. [1979] Attenuation of seismic waves in dry and saturated rocks, Laboratory measurements. *Geophysics* **44**, 681–690.
Tonn, R. [1991] The determination of seismic quality factor Q from VSP data: A comparison of different computational methods: *Geophys.Prosp.,* **39**, 1-27.
White, R, [1993] Discussion and reply to comment on "The accuracy of estimating Q from seismic data (short note) in *Geophysics* 57, 1508–1511". *The Leading Edge* **12**, 258.
Winkler, K. and Nur, A. [1979] Pore fluids and seismic attenuation in rocks. *Geophysical Research Letters* **6**, 1–4.
Wyllie, M.R.J., Gardner, G.H.F. and Gregory, A.R. [1962] Studies of elastic wave attenuation in porous media. *Geophysics* **27**, 569–589. (Addendum in *Geophysics* **28**, 1074)
Xu, C., Stewart, R. and Osborne, C. [2001[Walkaway VSP processing and Q estimation: Pikes Peak, Saskatchwan, presented at the *Annual CSEG Convention 2001*, Calgary.
Yilmaz, O. [2001] *Seismic Data Processing*. SEG Publication.